Hindawi
International Journal of Optics
Volume 2020, Article ID 9038053, 8 pages
https://doi.org/10.1155/2020/9038053

Research Article

Investigation of the Atmospheric Attenuation Factors in FSO Communication Systems Using the Taguchi Method

Pelin Demir and Güneş Yılmaz

Electrical- Electronics Engineering, Uludag University, Bursa 16059, Turkey

Correspondence should be addressed to Pelin Demir; pelinsule@gmail.com and Güneş Yılmaz; gunesy@uludag.edu.tr

Received 1 November 2019; Accepted 12 February 2020; Published 12 March 2020

Academic Editor: Giulio Cerullo

In this study, Mie and Rayleigh scattering in free space optics (FSO) communication systems were investigated in terms of the atmospheric attenuation. Because of the movement of the Earth, the communication distance and surrounding gas densities are inconsistent in each region. This change leads to atmospheric attenuation and then data losses and inefficient communication in FSO occur. Therefore, the density change and distance must be calculated in each communication once the data is transmitted. In the literature, it was observed that the atmospheric attenuation is regarding some FSO communication parameters such as transmission distance, visibility, and scatter particle size distribution, the number of particles per unit volume, scatter cross-sectional area, and wavelength. Besides, in real-time communication, it is necessary to update FSO parameters simultaneously. However, this updating process for all parameter takes a long time to adapt to a new position. This paper proposes the design of the experiment method (Doe) to determine the severity of the FSO parameters. And Taguchi's Doe method allows analyzing of FSO communication system parameters to avoid long calculation time. Results show that the proposed method helps in understanding the priorities of the parameters in FSO and reducing the updating time.

1. Introduction

Recently, free space optics (FSO) communication system has been a preferred communication system compared to radio frequency (RF). The advances in technology and increasing requirements have been contributed to the development of FSO communication system [1].

FSO communication provides high data rate, high transmission security, no frequency allocation, small size and low power requirement, and easy installation [2]. On the other hand, FSO communication systems have some disadvantages such as attenuation effects that lead to signal weakness and consequently limitation of transmission for communication. The attenuation effect of scattering and absorption causes a reduction in the performance because of affecting the laser beam. To obtain a better performance, the path between the receiver and the transmitter for FSO communication system should have a clean line of sight [3, 4]. Another attenuation effect is regarding the turbulence which occurs due to temperature and pressure fluctuations in the atmosphere. Furthermore, the weather conditions such as rain, snow, and fog lead to reducing the performance in the FSO communication system [5]. Also, the scintillation depending on the turbulence limits the data transmission speed and system performance in long-range communication [6].

Absorption and scattering occur due to particles which reduce both the turbulence and the optical signal, and thus lack of laser beam quality occurs [7]. Once Gaussian wave propagates through the atmospheric turbulence, the loss by scintillation is considered [8]. Due to the dimensions of particle, scattering types can be ranked as Rayleigh scattering, Mie scattering, and Geometry scattering [9]. By using fundamental modulation techniques, simple applications with low budget can be realized. Then, usage of On-Off Key (OOK) switching modulation enables the reduction of the fading effect [10].

While the laser beam propagates through the atmosphere, it is exposed to attenuation effects. To analyse the

attenuation effects, many calculations are required. These calculations are used for updating permeability equations, and this way, FSO communication systems are immune to variable atmospheric conditions. However, these calculations lead to time losses for data transmission. In this paper, Taguchi's experimental method is proposed to minimize the time losses and therefore enhance the performance of FSO communication systems and suppress the attenuation effects.

2. Atmospheric Properties

The atmosphere has many layers. These layers consist of different and variable gases. Figure 1 shows the gases' distribution in the atmospheric layers [11]. The troposphere layer shown in Figure 1 is about 15–20 km from the Earth and consists of the most intense gases because it is the closest layer to Earth.

In general, the percentages of gases in the atmosphere are as follows: 78% nitrogen, 20% oxygen, 9% argon, and 0.04% other gases (0.004%, 0.0018% Ne, 0.000524% He, 0.00018%, 0.00055%, 0.000114% Kr) [12]. Furthermore, each gas in the atmosphere has a different radius size. Due to the size of radius, the laser beam is affected in a different way when interacting with different gases. The laser beam is exposed to mostly nitrogen and oxygen during propagating in the atmosphere. The refractive indices and diameters of these gases for 1064 nm are given in Table 1. Gases such as Ne, CH_4, and Kr do not interact with the wavelength of 1064 nm. However, these gases are affected by different wavelengths.

2.1. Atmospheric Attenuation. According to the law of Beer, attenuation of laser beam propagation is given as

$$T = \frac{I(z)}{I_0} = \exp(-\gamma z), \tag{1}$$

where T is the permeability, γ is the attenuation coefficient, and z is the transmission length. The refractive index of gases at a certain wavelength consists of two parts which are real and virtual ($r = r' + r''$). In the near infrared region (NIR), the virtual part of the refractive index is small enough so as to be neglected. The virtual part of the refractive index defines scattering. Therefore, the attenuation due to the scattering can be considered. This way, the attenuation coefficient for scattering is shown as

$$\gamma = \beta_m + \beta_a, \tag{2}$$

where β is the scattering coefficient and indices of m and a represent the molecule and aerosol, respectively. Each coefficient in (2) depends on the wavelength of the laser emission [13]. There is no energy loss in case of scattering; however, the laser beam may be directed to any different location. So, this situation causes a decrease in beam intensity for long-distance transmissions. The physical size of the scatterers is a factor that determines scattering.

Air molecules lead to Rayleigh scattering in angstrom sizes. On the other hand, aerosols lead to Mie scattering because of scattering the light. The German meteorologist

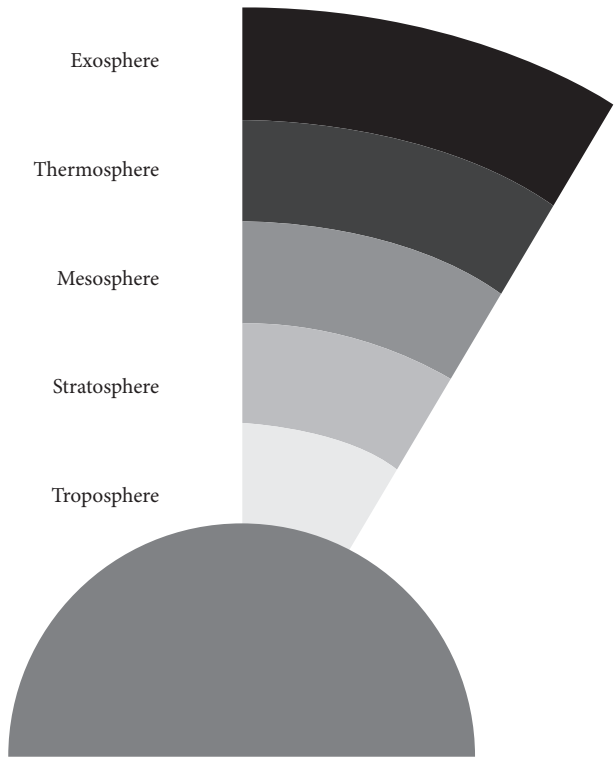

Figure 1: Atmospheric layers with gas distribution.

Gustav Mie found that electromagnetic waves are scattered by the small dielectric spheres. It is called Mie scattering [14].

Electrons which involve the formation of chemical bonds are called bonding electrons. Electronic displacement occurs when the electrons move towards the other side of the molecule. Once the bonding electrons are displaced, Rayleigh scattering occurs. The harmonic field stimulates the dipole in the molecule. Therefore, polarity of dipole determines where to move them. The propagation is absorbed, and the stimulated dipole oscillates at the same frequency with the laser beam. The radiated energy occurs by the scattering light. When a beam collides with a small particle, the area where the particle interacts with the beam is called the cross-sectional area. Total scattered cross-sectional area is given as [14]

$$\sigma = \frac{8\pi^3 (n^2 - 1)^2}{3N^2\lambda^4}, \tag{3}$$

where n is the refractive index and N is the scattered molecular density. Besides, aerosol scattering is known as Mie scattering which is shown as

$$\beta_a = \frac{3.91}{V}\left(\frac{\lambda}{550\,\text{nm}}\right)^{\rho}, \tag{4}$$

where V is the visibility, λ is the wavelength, and ρ is the size distribution of the scattering particles.

Different weather conditions can be specified based on their visibility range values. According to Kruse model, the relationship between the size distribution and visibility is determined using [15]

Table 1: Refractive indices and diameters of atmospheric gases.

Gas	Refractive index ($\lambda = 850$ nm)	Refractive index ($\lambda = 1064$ nm)	Refractive index ($\lambda = 1550$ nm)	Diameter (pm)
N_2	1.00029596	1.0002952	1.00029442	112
O_2	1.00024932	1.0002484	1.00024763	96
Ar	1.00027950	1.0002820	1.00027808	142
CO_2	1.00044397	1.0004419	1.00043822	232.42
Ne	1.00006610 (0.5462 μm)	1.00006610 (0.5462 μm)	1.00006610 (0.5462 μm)	76
He	1.000034787	1.00003475	1.000034708	62
CH_4	1.0004365 (1.68 μm)	1.0004365 (1.68 μm)	1.0004365 (1.68 μm)	398
H_2	1.00013718	1.0001367	1.00013617	102
Kr	1.0004266 (0.6234 μm)	1.0004266 (0.6234 μm)	1.0004266 (0.6234 μm)	170
H_2O	1.3290	1.3260	1.3180	94.2

$$p = \begin{pmatrix} 1.6 & V > 50\,\text{km} \\ 1.3 & 6\,\text{km} < V < 50\,\text{km} \\ 0.585V^{1/3} & V < 6\,\text{km} \end{pmatrix}. \quad (5)$$

Rayleigh scattering is also known as molecular scattering. For a single molecule, it is given as

$$\beta_m = 0.827 N_p A_p \lambda^{-4}, \quad (6)$$

where N_p is the number of particles per unit volume and A_p is the cross-sectional area of scattering. Also, A_p is given as [16]

$$A_p = \pi r^2, \quad (7)$$

where r is the radius of the mass for a molecule. In the atmosphere according to the geological location, the particle size distribution and concentration vary. Visibility must also be taken into account when calculating aerosol scattering. So, they must be known while calculating the aerosol scattering [17].

Also, the aerosol size distribution depends on relative humidity and wind speed. Humidity affects the active refractive index of the aerosol particle. In this case, two different particle distributions are taken into account as continental and maritime air. In hazy weather conditions with 5 km visibility, absorption and extinction coefficients are increased by 4.87 multiplier factors [18].

3. Taguchi Optimization Method

Taguchi method is useful in determining the optimum combination results for any system [19]. This method was firstly used in quality engineering and product design studies, and today, it is used in various studies which are trying to reach the result by doing less experimentation or analyses [20]. The difference between the Taguchi method and other statistical methods is that it allows grouping controlled and uncontrollable parameters, and therefore it provides analyzing for multiple parameters in the case of more than two levels. Furthermore, it minimizes the variance in the target area while bringing the average of performance value to the desired level [21]. The Taguchi method is based on the orthogonal arrays [22]. And it is widely used to design experimental studies. The optimal number of experiments can be achieved by Taguchi optimization method, and the control parameters are determined by using orthogonal arrays (OA) [23, 24]. Figure 2 shows the flow chart for Taguchi's method which consists of five steps in general approach. These steps are concerning defining the parameters and its level of system, selection of orthogonal array, creating your experimental table, calculating the result and ranking priority of parameters, and finally eliminating the unnecessary parameters with low severity.

Each system or embodiment consists of some parameters which have some values. The value of parameter is called level in Taguchi's method. The right design of experiment must be defined for a suitable solution. The selection matrix in Taguchi's method is given in Table 2. According to the number of parameters and the level of each parameter, a suitable experiment table can be selected by using Table 2 [23].

3.1. Theoretical Method. In the theoretical study, wavelengths of 850 nm and 1064 nm were used for analysis. Visibility value was used as 6 km in calculations. For each wavelength, Mie and Rayleigh attenuation were calculated by using (6) and (7) and N_p and A_p are calculated for each gas as shown in Table 3.

While calculating the A_p value, r parameter is obtained [26]:

$$r = r_0 A^{1/3}, \quad (8)$$

where r is the radius of the nucleus of mass number A and the parameter r_0 is constant and its value is 1.2×10^{-15} m.

Considering Table 3, the calculated Rayleigh scattering values for 850 nm and 1064 nm are shown in Table 4.

As shown in Table 4, the scattering values were calculated for each gas in the troposphere, as the value of visibility is to be considered 6 km for the troposphere. The ratio of gas and diversity of gas are more at the troposphere. The scattering behaviour at two different wavelengths was observed for wavelength of 850 nm and 1064 nm. Rayleigh scattering occurs more under the same conditions which is 850 nm wavelength.

The shorter end of the visible spectrum is closer to oxygen and nitrogen gases as an atom, and they interact more and scatter to a higher degree. Therefore, a shorter wavelength of light scatters more than longer wavelengths.

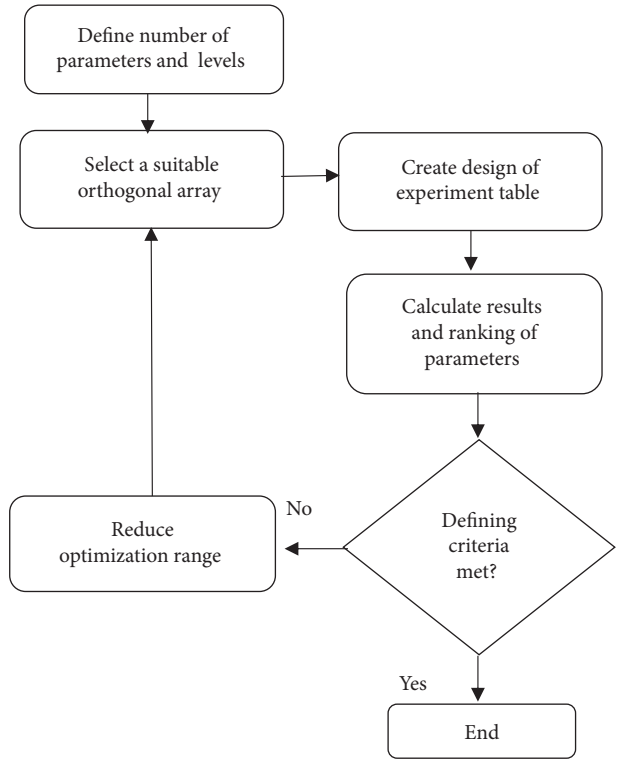

Figure 2: General Taguchi's method approach [25].

Table 2: Taguchi orthogonal array selection matrix [23].

		Parameter number											
		4	5	6	7	8	9	10	11	12	13	14	15
	2	L8	L8	L8	L8	L12	L12	L12	L12	L16	L16	L16	L16
Level number	3	L9	L18	L18	L18	L18	L27	L27	L27	L27	L27	L36	L36
	4	L′16	L′16	L′32	L′32	L′32	L′32	L′32					

Table 3: Number of gas molecules in the atmosphere.

Gas	Number of molecules per unit volume N_p	Cross-section area A_p
N_2	3.3×10^{21}	4.162×10^{-23}
O_2	8.8×10^{20}	4.441×10^{-23}
Ar	4.2×10^{19}	5.178×10^{-23}
CO_2	1.7×10^{18}	5.621×10^{-23}
Ne	8.1×10^{15}	3.318×10^{-23}
He	2.2×10^{17}	1.138×10^{-23}
CH_4	8.1×10^{15}	2.870×10^{-23}
H_2	2.2×10^{15}	7.172×10^{-24}
Kr	4.5×10^{15}	8.593×10^{-23}

Table 4: Rayleigh scattering values for 850 nm and 1064 nm.

Gas	850 nm Rayleigh scattering	1064 nm Rayleigh scattering
N_2	0.2169	0.0886
O_2	0.0617	0.02521
Ar	3.435×10^{-3}	1.4010×10^{-3}
CO_2	1.509310^{-4}	6.1655×10^{-5}
Ne	4.24×10^{-7}	1.7340×10^{-7}
He	3.9546×10^{-6}	1.6153×10^{-6}
CH_4	3.6720×10^{-7}	1.499×10^{-7}
H_2	2.4923×10^{-8}	1.0180×10^{-8}
Kr	6.1079×10^{-7}	2.4949×10^{-7}

Table 5: Mie scattering values for 850 nm and 1064 nm.

Visibility (km)	850 nm Mie scattering	1064 nm Mie scattering
$V > 50$	0.4724	42
$6 < V$ (15) <50	0.2243	1.3855
$V < 6$	0.0506	0.4784

As shown in Table 5, the Mie scattering values are calculated by (4) with different visibilities.

The result of the obtained values can be evaluated with the graphs as given in Figures 3 and 4. Figure 3 shows the attenuation values of each gas molecule for 850 nm at a distance of 6 km from the Earth. It is seen that the nitrogen value has the highest value and then comes oxygen. The attenuation rates of other gases are close to each other. Figure 4 shows the attenuation values for 1064 nm. Oxygen and argon were the prominent gas molecules at 1064 nm with respect to 850 nm.

As a result, total attenuation is increased at larger wavelengths in the case of low-visibility weather conditions

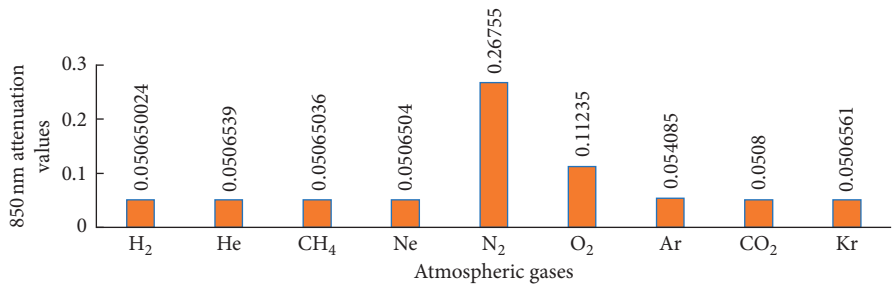

Figure 3: Attenuation values for 850 nm.

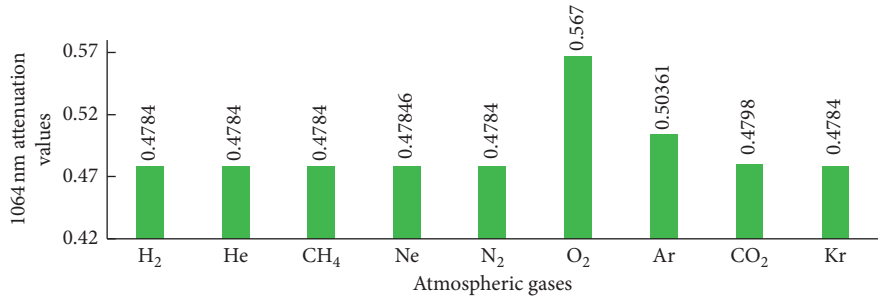

Figure 4: Attenuation values for 1064 nm.

($V = 6$ km). Besides, total attenuation for larger wavelength increases in the case of high visibility clean air conditions ($V = 50$ km).

Once any visibility condition is concerned, it is understood that increasing of the total attenuation is independent from the wave length.

By using a different wavelength, the total attenuation value of N_2 at 1550 nm is ~20.6, and this value is greater than the attenuation values for the wavelengths of 980 nm and 1064 nm. The selection of wavelength happens according to the material which produces laser. 1550 nm, 1064 nm, and 980 nm wavelengths are obtained by VCSEL solid state pulsed type laser, Nd YAG type laser, and InGaAs type laser, respectively. The data rate of the 1550 nm and 1064 nm wavelength laser is about 10 Gbps, and for 980 nm it is 1-2 Gbps [27].

The data rate of wavelength with maximum attenuation is higher than the other wavelengths. However, this requires the determination of the severity for the attenuation parameters.

Because, the attenuation at 1550 nm leads to transmitting more power to overcome the attenuation due to fog, smoke, cloud, and so on. In this case, the severity for the parameters for attenuation must be determined by using Taguchi method.

3.2. Taguchi's Design of Experiment in Free Space Optics Communication. Firstly, the orthogonal array has been selected, and then the other step is to determine the input parameters. Response table is formed by the values obtained as a result of the iteration. When the experiments are carried out and the iteration is completed, a test chart is created with the results obtained. Figure 5 shows the diagram of the proposed method.

In this section, lower and upper limits were determined for the six parameters related to attenuation values due to Rayleigh and Mie scattering which are atmospheric effects in free space optics communication as shown in Tables 4 and 5. The values of the two levels for upper and lower limits are given in Table 6.

The selected parameters are directly related to the attenuation coefficient.

Considering the six parameters and two levels for atmospheric attenuation, appropriate orthogonal array is L8 experiments in Table 2. Experimental design chart for L8 is created by using Table 6 and orthogonal sequence selection matrix of Taguchi method is shown in Table 7.

4. Results and Discussion

This paper proposes to use Taguchi's design of experimental method. In this context, six parameters and their two levels (considering the minimum and maximum values) were considered to define orthogonal experiment array which is suitable for L8 shown in Table 2. So, L8 orthogonal array has eight experiments shown in Table 7. By using the attenuation equations for the atmosphere, Rayleigh and Mie, the experiments (calculations) shown in Table 7 were performed. The obtained results for attenuation are shown in Table 8.

Another step is the calculation of the signal noise ratio (SNR) in Taguchi's method. SNR values are calculated for all levels of defined parameters so as to get absolute delta between minimum and maximum SNR values for these parameter levels. This way, the parameters effect on the attenuation can be ranked according to their priority levels. Therefore, it allows having a chance to eliminate an unnecessary parameter or a parameter with low effect on attenuation. SNR values for the obtained values are shown in

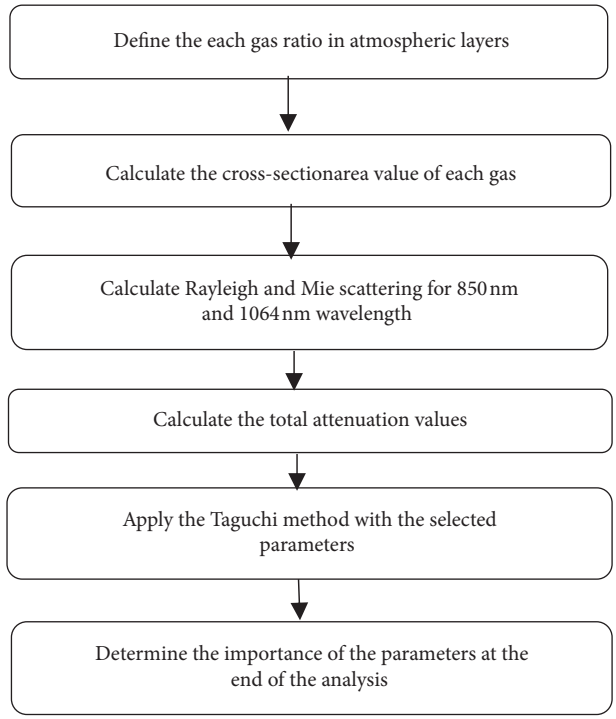

Figure 5: The diagram of the proposed method.

Table 6: Free space optics communication scattering and absorption parameters experimental design levels.

Parameters	Level I	Level II
Transmission distance (L)	1 km	12 km
Visibility (V)	6 km	50 km
Scatter particle size distribution (p)	1.3	1.6
Number of particles per unit volume (N_p)	2.2×10^{15} (H_2)	3.3×10^{21} (N_2)
Scatter cross-sectional area (A_p)	7.172×10^{-24}	8.593×10^{-23}
Wavelength (λ)	850 nm	1064 nm

Table 7: Free space optics attenuation experiment design chart for L8.

Experiments	Transmission distance (km)	Visibility (km)	Scatter particle size distribution	Number of particles per unit volume	Scatter cross- sectional area	Wavelength (nm)
1	1	6	1.3	2.2×10^{15} (H_2)	7.172×10^{-24}	850
2	1	6	1.3	3.3×10^{21} (N_2)	8.593×10^{-23}	1064
3	1	50	1.6	2.2×10^{15} (H_2)	7.172×10^{-24}	1064
4	1	50	1.6	3.3×10^{21} (N_2)	8.593×10^{-23}	850
5	12	6	1.6	2.2×10^{15} (H_2)	8.593×10^{-23}	850
6	12	6	1.6	3.3×10^{21} (N_2)	7.172×10^{-24}	1064
7	12	50	1.3	2.2×10^{15} (H_2)	8.593×10^{-23}	1064
8	12	50	1.3	3.3×10^{21} (N_2)	7.172×10^{-24}	850

Table 8: Results using Taguchi analysis.

Experiments	Results
1	0.319
2	$3.30E-80$
3	$1.67E-06$
4	$1.00E-150$
5	0.151
6	$2.53E-89$
7	0.109
8	$1.00E-100$

Table 8. Absolute delta values between minimum and maximum parameter levels and parameters ranking are given in Table 9.

According to Table 9, the scatter cross-sectional area is the most important parameter. Visibility and scatter particle size distribution then follow.

The analysis result shows that the most important parameter is the scatter cross-sectional area Ap which directly affects Rayleigh scattering. The effect of Rayleigh scattering to the attenuation parameter appears to be bigger than Mie

Table 9: Analysis result and importance level.

Parameters	Level 1	Level 2	Delta	Ranking
Transmission distance	−1083.910	−1009.626	74.284	6.00
Visibility	−746.870	−1596.119	849.249	2.00
Scatter particle size distribution	−1533.185	−784.631	748.554	3.00
Number of particles per unit volume	−1199.851	−984.631	215.220	5.00
Scatter cross-sectional area	−681.433	−1705.182	1023.74	1.00
Wavelength	−786.180	−1344.497	558.317	4.00

scattering. This analysis may indicate that Mie scattering can be neglected for a satellite placed on the troposphere.

Considering the wavelength together with visibility, it can be neglected in low visibility. In the low-visibility for communication at the troposphere distance, compared to the selected wavelengths such as 850 nm, 1064 nm, and 1550 nm, the best result is taken for 850 nm.

While designing FSO communication system, atmospheric events can be estimated and the wavelength to be transmitted can be selected. Thus, more efficient and fast communication will be ensured.

Under these conditions, the number of experiments is reduced by using the selected "six" parameters. Taguchi method allows the elimination of the parameters with low importance and therefore the approximate result would be obtained in a shorter time.

5. Conclusions

According to the analysis, the scattering cross-sectional area of the gas particles directly affects the attenuation.

The results of analysis show that N_2 gases at 850 nm wavelength and O_2 gases at 1064 nm wavelength affect significantly the scattering. The reason for these obtained findings depends on the particle dimension of N_2 and O_2 gases. Therefore, Taguchi analysis was used for investigating the effect of these gases on the scattering.

Taguchi method allowed the reduction of the number of experiments and saving analysis time. The Taguchi method has shown that eight experiments for assessment are satisfactory compared to 64 experiments in the case of six parameters and two levels.

Due to the movement of the Earth, the communication distance and surrounding gas densities are changeable in each region. From this change, the density change and distance should be calculated in each communication when the data is transmitted. These calculations lead to too many experiments to determine the desired parameters. Taguchi method reduces the number of experiments by calculating the most important parameters and thus saves time. Taguchi method for FSO systems was found to be a useful method for analysis.

Data Availability

The data used to support the findings of this study are included within the article.

Conflicts of Interest

The authors declare that they have no conflicts of interest.

References

[1] A. Malik and P. Singh, "Free space optics: current applications and future challenges," *International Journal of Optics*, vol. 2015, Article ID 945483, 7 pages, 2015.

[2] M. H. Mahdieh and M. Pournoury, "Atmospheric turbulence and numerical evaluation of bit error rate (BER) in free-space communication," *Optics & Laser Technology*, vol. 42, no. 1, pp. 55–60, 2010.

[3] A. K. Majumdar and J. C. Ricklin, *Free Space Laser Communications*, John Wiley and Sons, New York, NY, USA, 2008.

[4] G. Alnwaimi, H. Boujemaa, and K. Arshad, "Optimal packet length for free-space optical communications with average SNR feedback channel," *Journal of Computer Networks and Communications*, vol. 2019, Article ID 4703284, 8 pages, 2019.

[5] H. Yuksel, *Studies of the effects of atmospheric turbulence on free space optical communications*, Department of Electrical and Computer Engineering, University of Maryland, College Park, MD, USA, Ph.D. dissertation, 2005.

[6] S. Navidpour, M. Uysal, and M. Kavehrad, "BER performance of free-space optical transmission with spatial diversity," *IEEE Transactions on Wireless Communications*, vol. 6, no. 8, pp. 2813–2819, 2007.

[7] A. K. Majumdar, *Advanced Free Space Optics (FSO) a Systems Approach*, Springer, Atlanta, GA, USA, 2015.

[8] A. ElHelaly, A. H. Mehana, and M. M. Khairy, "Reduced-complexity receiver for free-space optical communication over orbital angular momentum partial-pattern modes," *International Journal of Antennas and Propagation*, vol. 2018, Article ID 8514705, 11 pages, 2018.

[9] A. S. El-Wakeel, N. A. Mohammed, and M. H. Aly, "Free space optical communications system performance under atmospheric scattering and turbulence for 850 and 1550 nm operation," *Applied Optics*, vol. 55, no. 26, pp. 7276–7286, 2016.

[10] K. O. Odeyemi, P. A. Owolawi, and V. M. Srivastava, "Performance analysis of free space optical system with spatial modulation and diversity combiners over the gamma gamma atmospheric turbulence," *Optics Communications*, vol. 382, no. 1, pp. 205–211, 2017.

[11] D. R. Lide, *Handbook of Chemistry and Physics*, CRC Press, Boca Raton, FL, USA, 84th edition, 2003.

[12] F. Möller, "Optics of the lower atmosphere," *Applied Optics*, vol. 3, no. 2, pp. 157–166, 1964.

[13] A. Bucholtz, "Rayleigh-scattering calculations for the terrestrial atmosphere," *Applied Optics*, vol. 34, no. 15, pp. 2765–2773, 1995.

[14] O. Bouchet, H. Sizun, C. Boisrober, F. Forne, and L. P. N. Favennec, *Free-Space Optics Propagation and Communication*, ISTE Ltd., London, UK, 2006.

[15] X. Chen, X. Gao, X. Qu et al., "Qualitative simulation of photon transport in free space based on monte carlo method and its parallel implementation," *International Journal of*

Biomedical Imaging, vol. 2010, Article ID 650298, 9 pages, 2010.

[16] H. Weichel, "Atmospheric propagation of laser beams," *SPIE*, vol. 547, no. 1, pp. 1–15, 1985.

[17] G. Taguchi and Y. W. S. Chowdhury, *Taguchi's Quality Engineering Handbook Architecture*, Wiley, New York, NY, USA, 2005.

[18] B. Gökçe and S. Tasgetiren, "A system development for the design and optimization of metallurgical experiments by using genetic algorithms and taguchi methods," *Journal of Scientific and Industrial Research*, vol. 73, pp. 219–224, 2014.

[19] T. T. K. Elfarah, *Magnezyum matrisli karbür takviyeli kompozitlerin toz metalurjisi yöntemi ile üretiminin Taguchi metodu ile optimizasyonu*, Dept of Mate. And Scien. Eng., Kastamanu Univ., Kastamonu, Turkey, Ph.D. dissertation, 2018.

[20] C. R. Rao, "Factorial experiments derivable from combinatorial arrangements of arrays," *Supplement to the Journal of the Royal Statistical Society*, vol. 9, no. 1, pp. 128–139, 1947.

[21] W. Weng, F. Yang, and A. Elsherbeni, *Electromagnetics and Antenna Optimization Using Taguchi's Method*, Morgan & Claypool Pub, San Rafael, CA, USA, 1st edition, 2007.

[22] U. Demir and M. C. Aküner, "Using Taguchi method in defining critical rotor pole data of LSPMSM considering the power factor and efficiency," *Tehnicki Vjesnik—Technical Gazette*, vol. 24, no. 2, pp. 347–353, 2017.

[23] U. Demir and M. C. Aküner, "Design and optimization of in-wheel asynchronous motor for electric vehicle," *Journal of the Faculty of Engineering and Architecture of Gazi University*, vol. 33, no. 4, pp. 1517–1530, 2018.

[24] H. Haroon, H. A. Razak, S. S. Khalid, N. Nadia, and A. Aziz, "On the effectiveness of Taguchi method in optimizing the performance of parallel cascaded MRR array (PCMRRA)," *Optoelectronics and Advanced Materials*, vol. 11, no. 7-8, pp. 393–397, 2017.

[25] W.-C. Weng, F. Yang, and A. Z. Elsherbeni, "Linear antenna array synthesis using Taguchi's method: a novel optimization technique in electromagnetics," *IEEE Transactions on Antennas and Propagation*, vol. 55, no. 3, pp. 723–730, 2007.

[26] Nuclear Size and Density, CR Nave, USA, 2000, http://hyperphysics.phy-astr.gsu.edu/.

[27] H. Kaushal, V. K. Jain, and S. Kar, "Free space optical communication," in *Optical Networks*, Springer, Berlin, Germany, 2017.